On Line Supplemental Material:

A) Materials and Methods

B) Supplemental Tables 1-3

C) Supplemental Figures and Figure Legends

D) References

Materials and Methods:

Animals and in vivo Study Design

Mice expressing the PKG1α C42S mutant as a global knock-in were generated in the C57Bl/6 background as described (1), and used along with littermate controls. All procedures were performed in accordance with institutional and NIH guidelines for the care and use of animals in biomedical research, and approved by the Johns Hopkins Medical Institutions Animal Care and Use Committee.

Pressure-overload (Trans-aortic constriction; TAC)

Male mice (4 months age) and matched for body size were randomly assigned to surgery groups and TAC surgery(2) performed by an individual blinded to the genotype. Surgery was performed under isoflurane anesthesia, with a 7-0 prolene suture placed around the transverse aorta, the constriction sized using a 27-gauge needle (2). Controls were subjected to sham operations, and animals were studied 1 to 3 wk after surgery. *In vivo* analysis and post-sacrifice myocardial histological and molecular analysis was performed blinded as to experimental group.

Echocardiography

In vivo cardiac morphology/function was assessed by a technician blinded as to the experimental condition, using transthoracic echocardiography (Acuson Sequoia C256, 13-MHz; Siemens) in conscious mice. M-mode images provided measures of wall thickness, end-systolic and end-diastolic dimensions, fractional shortening, and LV mass, each determined from an average of 3-5 beats.

Human Cardiac Samples

Human heart tissue specimens were obtained in accordance with Institutional Review Board approval at the University of Pennsylvania and Johns Hopkins University, and consent for research use of

explanted tissues was obtained prospectively in all cases. Failing human hearts were procured at the time of orthotopic heart transplantation at the Hospital of University of Pennsylvania. Nonfailing hearts were obtained at the time organ donation from cadaveric donors. In all cases, hearts were arrested in situ using ice-cold cardioplegia solution, transported on wet ice, and flash frozen in liquid nitrogen within four hours of explantation. All samples were full-thickness biopsies obtained from the free wall of the left ventricle.

Tissue Histology

Myocardium fixed in 10% paraformaldehyde overnight was embedded in paraffin, sectioned in 10-µm slices, and stained with hematoxylin/eosin or Masson's trichrome to analyze interstitial fibrosis. Six serial mid-LV sections per heart, at the level of papillary muscle was quantified using computer-assisted image analysis (Adobe Photoshop version 5.0). Tissue was also stained with wheat germ agglutinin (WGA, Alexa Fluor 488 conjugated) to assess cardiomyocyte hypertrophy. The images were captured with fluorescence microscopy and cardiomyocyte cross sectional area (CSA) quantified with 400-600 cells per heart, using NIH Image J. Histological analysis was performed blinded to the tissue source.

Measurement of myocardial ROS

Tissue levels of reduced (GSH) and oxidized glutathione (GSSG) and of malondialdehyde (MDA) and 4-hydroxyalkenals (4-HAE) were determined (Bioxytech GSH/GSSG-412 kit or LPO-586 kit; Oxis Health Products, Inc.) following manufacturer's instructions (3, 4).

Protein analysis

Lysates were prepared with lysis buffer (Cell Signaling Technology) from snap-frozen heart tissue or cardiac myocytes isolated from adult mice or neonatal rats. For non-reducing SDS PAGE, 100 mM N-

ethylmaleimide (SIGMA) was added to the lysis buffer to prevent artificial thiol oxidation during sample preparation. Samples under non-reducing conditions were prepared by mixing SDS sample buffer without adding DTT(5). Protein concentrations were measured by BCA method (Pierce). All protein extracts were run on Novex Tris-Glycine Gels (Life Technologies), then blotted onto nitrocellulose membranes, and probed with various primary antibodies (On Line supplement – Table 2). All antibodies were from Cell Signaling Technology, except for monoclonal anti-FLAG M2 antibody (Sigma-Aldrich) and PKG1α specific antibody generously provided by Robert Blanton (Division of Cardiology, Tufts University). Antibody binding was visualized with an infrared imaging system (Odyssey, Licor) and quantification of band intensity performed using Odyssey Application Software 3.0. To calculate the percentage of dimeric PKG1α, the intensity of the dimer band was normalized to the sum of monomer+disulfide band intensities taken from the same gel lane (sample). These ratios were then compared by non-parametric test (Mann-Whitney).

Quantitative real-time PCR

Total RNA was extracted with Trizol Reagent (Invitrogen), then reverse transcribed into cDNA using a High Capacity RNA-to-cDNA Kit (Applied Biosystems, Life technologies). cDNA was subjected to PCR amplification using either TaqMan or SYBR green with specific primers for target sequences or gylceraldehyde-3-phosphate dehydrogenase (GAPDH) (On Line Supplemental Table 3). The threshold cycle (Ct) value, which was determined using crossing point method, was normalized to GAPDH (Applied Biosystems, California, U.S.A) Ct value in each run.

In vitro PKG activity and cyclic nucleotide assay

In vitro PKG activity was assayed in both heart tissues subjected to Sham or TAC and neonatal rat myocytes which were incubated with ET-1, PE, H_2O_2 alone, or cGMP in the presence of H_2O_2, using a colorimetric assay (Cyclex) as described (2, 6). This assay provides a single non-limiting concentration of kinase substrate (thus, affinity binding changes, e.g. K_m are not assessed), with cGMP and ATP added to

the incubation buffer in a timed reaction. Most runs of the assay included cGMP in the reaction buffer as per manufacture's instructions; however, we also performed the assay in the absence of cGMP to determine the latter's effect on detecting redox-mediated kinase activation.

Myocardial cGMP was assessed in hearts homogenized in 6 % trichloroacetic acid, centrifuged and extracted with water-saturated ether. The aqueous phase was transferred, vacuum dried, and pellet resuspended in sodium acetate buffer for cGMP enzyme immunoassay (Amersham Pharmacia Biotech).

Adult mouse cardiac myocytes (AMCMs) immunohistochemistry and cell fractionation analyses

AMCMs were isolated, fixed, and stained for confocal microscopy as described previously. Cells were plated on laminin-coated imaging dishes, and incubated in Tyrode's solution with 10 μM of hydrogen peroxide. Cells were fixed with ice-cold 50 % v/v methanol and 50 % v/v acetone, permeabilized with 0.1% saponin in PBS, blocked in 10% FBS in PBS, incubated with primary antibodies at 4 ^{o}C overnight (anti-PKG1α; anti-FLAG), and then subsequently incubated with secondary antibody (Alexa Fluor 488-conjugated goat anti-rabbit; Alexa Fluor 488-conjugated goat anti-mouse). Imaging was performed on Zeiss inverted epifluorescent microscope (Carl Zeiss Inc.) attached to an argon-krypton laser confocal scanning microscope (UltraView; Perkin Elmer Life Science Inc.)(7). Fractionation from isolated AMCMs was performed as described (7).

Myocyte culture studies

Recombinant adenoviruses of human wild-type N-terminal FLAG-tagged PKG1α and the Cys42Ser mutant were generated with DNA constructs subcloned into the multiple cloning site (Bgl II/XhoI) of the adenoviral shuttle vector pADTrackCMV. Recombinant adenoviruses for human TRPC6 and TRPC6 with the PKG-phosphorylation sites (T70A and S322Q) mutated, were generated from pcDNA3-human TRPC6-YFP. Primary cultures of neonatal rat cardiomyocytes were prepared as described(8). After overnight culture, NRCMs were infected with adenovirus (AdV) wild-type or C42S PKG1α, or co-infected with AdV

PKG1α (WT or C42S) and AdV TRPC6 (control or phospho-silencing mutant TRPC6). Co-transfection with indicated siRNA, was performed using Lipofectamine 2000 (Life Technologies) after AdV PKG1α infection, following the manufacturer's protocol. Twenty-four hours after transfection, cells were stimulated with Gq agonists (10 nM ET1 or 10μM PE) in serum-free DMEM media supplemented with 0.1% Insulin-Transferrin-Selenium (Life Technologies). RNA or protein was harvested 48 hours after stimulation. Exogenous PKG1α in NRCMs was detected using a FLAG antibody.

Statistical analysis

All values are presented as mean ± SEM. Group comparisons were performed by 1- or 2-way ANOVA or repeated measures ANOVA as required, using a Tukey post-hoc multiple comparisons test. Normality and equal-variance testing was performed for all ANOVA assays, and if the data failed this test, a non-parametric analysis (Mann-Whitney (2-groups) or Kruskal-Wallis (>2 groups) was performed. For all studies, experiments were performed 2-3 times, each involving n=3-7 per group (molecular samples from a given heart, or animal). For *in vivo* animal studies, ~10-20 animals were analyzed per group, a sample size overpowered to detect functional differences, but required to provide sufficient cardiac material for the various molecular and other assays. Sample sizes and individual statistical results are provided in the figures, supplemental figures, or each figure legend.

Supplemental Table S1. Clinical characteristics of patients with non-failing (donor) versus failing ventricles. The latter group all had diffuse ischemic heart disease.

		Non-Failing Controls (n=8)	Heart Failure (n=8)	p-value
Age	Yrs	54 ± 8.7	59 ± 6.0	0.15
Sex	M/F	8/0	8/0	NS
Heart Weight	gm	416.1 ± 66.8	707.9 ± 171	<0.001
Heart/Body Weight	gm/kg	5.1 ± 0.9	8.2 ± 1.6	<0.001
Bi-ventricular Pacing		0/8	7/8	0.001
Prior CABG		0/8	1/8	>0.5
Beta Blocker		3/7	7/8	0.12
Ejection Fraction	%	66 ± 6.6	13.1 ± 4.6	<0.001
Systolic BP	mmHg	129 ± 10.1	101 ± 14.3	<0.005
Diastolic BP	mmHg	79 ± 14.6	62.4 ± 15.3	0.1

Statistical Analysis: unpaired t-test for parametric variables, 2x2 table Fischer Exact Test for descriptive variables.

Supplemental Table S2. Antibodies for western blot analysis and immunocytochemistry

Antibody	Company	Catalog Number
Pan-Calcineurin A	Cell Signaling Technology, Inc	#2614
CaMKII	Cell Signaling Technology, Inc	#3362
p-CaMKII (T286)	Cell Signaling Technology, Inc	#3361
Akt	Cell Signaling Technology, Inc	#9272
p-Akt (S473)	Cell Signaling Technology, Inc	#4060
ERK1/2	Cell Signaling Technology, Inc	#9102
p-ERK1/2 (T202/Y204)	Cell Signaling Technology, Inc	#4370
GAPDH	Cell Signaling Technology, Inc	#2118
α-Tubulin	Cell Signaling Technology, Inc	#3873
FLAG M2	Sigma-Aldrich	#F1804

Supplemental Table S3. Primers for real-time PCR assays

Species/Gene (SYBR Green Primers)	Sequences (F/R)
Mouse Nppa	5’-TCGTCTTGGCCTTTTGGCT-3’ (Forward)
	5’-TCCAGGTGGTCTAGCAGGTTCT-3’ (Reverse)
Mouse Nppb	5’- AAGTCCTAGCCAGTCTCCAGA-3’ (Forward)
	5’- GAGCTGTCTCTGGGCCATTTC-3’ (Reverse)
Mouse βMHC (Myh7)	5’- ATGTGCCGGACCTTGGAAG-3’ (Forward)
	5’- CCTCGGGTTAGCTGAGAGATCA-3’ (Reverse)
Rat Nppa	5’- ATCTGATGGATTTCAAGAACC-3’ (Forward)
	5’-CTCTGAGACGGGTTGACTTC-3’ (Reverse)
Rat Nppb	5’- ACAATCCACGATGCAGAAGCT-3’ (Forward)
	5’- GGGCCTTGGTCCTTTGAGA-3’ (Reverse)
Rat GAPDH	5’- GACATGCCGCCTGGAGAAAC-3’ (Forward)
	5’- AGCCCAGGATGCCCTTTAGT-3’ (Reverse)

Species/Gene (TaqMan Primers)	Acc No.
Mouse Rcan-1	Mm01213407_m1
Mouse GAPDH	Mm99999915_m1
Rat Rcan-1	Rn00596606_m1
Rat RGS2	Rn00584932_m1
Rat RGS4	Rn00568067_m1

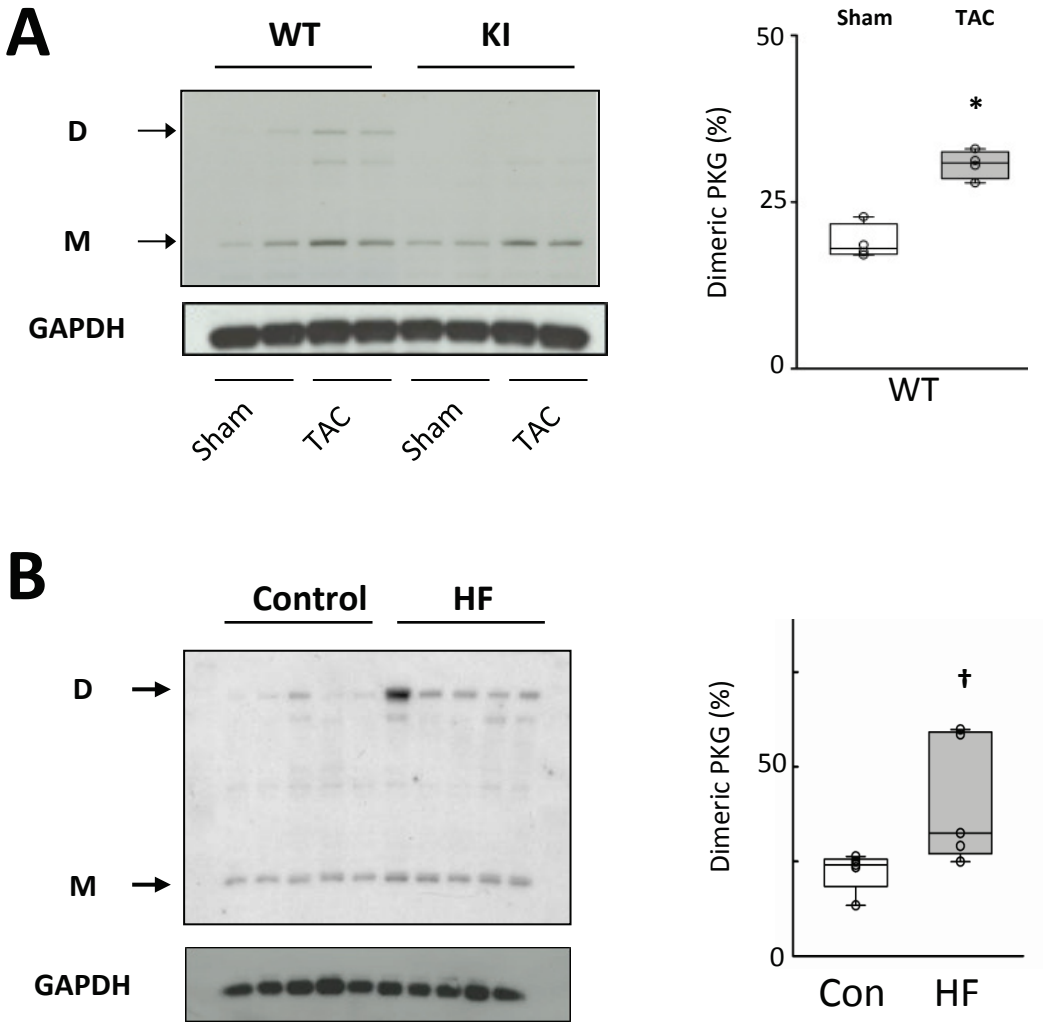
A
WT
KI
D
M
GAPDH
Sham
TAC
Sham
TAC
Sham
TAC
50
25
0
Dimeric PKG (%)
*
WT
B
Control
HF
D
M
GAPDH
50
0
Dimeric PKG (%)
†
Con
HF

Figure S1

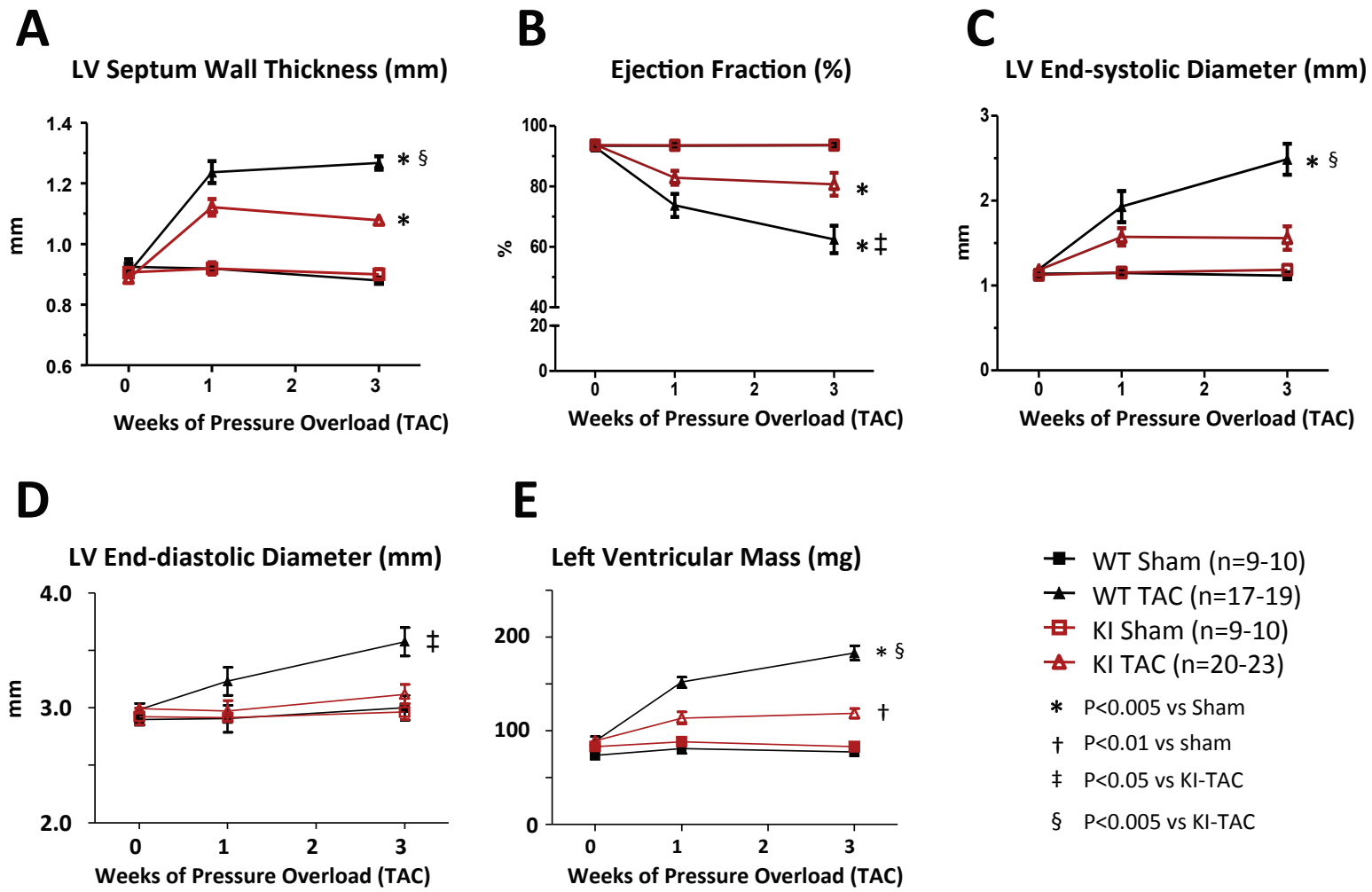
A
LV Septum Wall Thickness (mm)
mm
1.4
1.2
1.0
0.8
0.6
0
1
2
3
Weeks of Pressure Overload (TAC)
* §
*
B
Ejection Fraction (%)
%
100
80
60
40
20
0
Weeks of Pressure Overload (TAC)
*
* ‡
C
LV End-systolic Diameter (mm)
mm
3
2
1
0
Weeks of Pressure Overload (TAC)
* §
D
LV End-diastolic Diameter (mm)
mm
4.0
3.0
2.0
Weeks of Pressure Overload (TAC)
‡
E
Left Ventricular Mass (mg)
200
100
0
Weeks of Pressure Overload (TAC)
* §
†
WT Sham (n=9-10)
WT TAC (n=17-19)
KI Sham (n=9-10)
KI TAC (n=20-23)
* P<0.005 vs Sham
† P<0.01 vs sham
‡ P<0.05 vs KI-TAC
§ P<0.005 vs KI-TAC

Figure S2

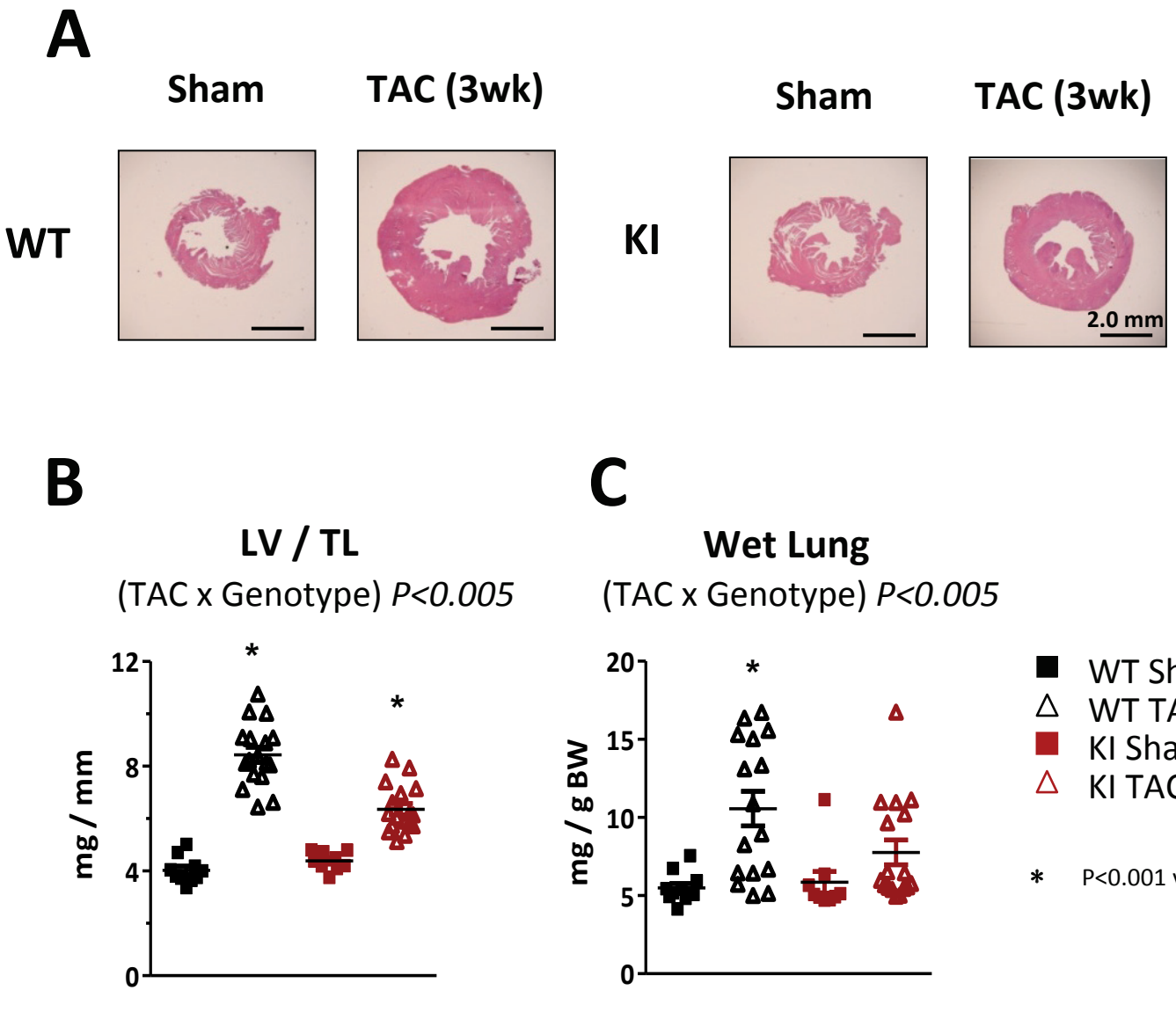
A
Sham
TAC (3wk)
Sham
TAC (3wk)
WT
KI
2.0 mm
B
LV / TL
(TAC x Genotype) P<0.005
mg / mm
12
8
4
0
*
*
C
Wet Lung
(TAC x Genotype) P<0.005
mg / g BW
20
15
10
5
0
*
WT Sham (n=10)
WT TAC (n=16)
KI Sham (n=9)
KI TAC (n=17)
* P<0.001 vs Sham

Figure S3

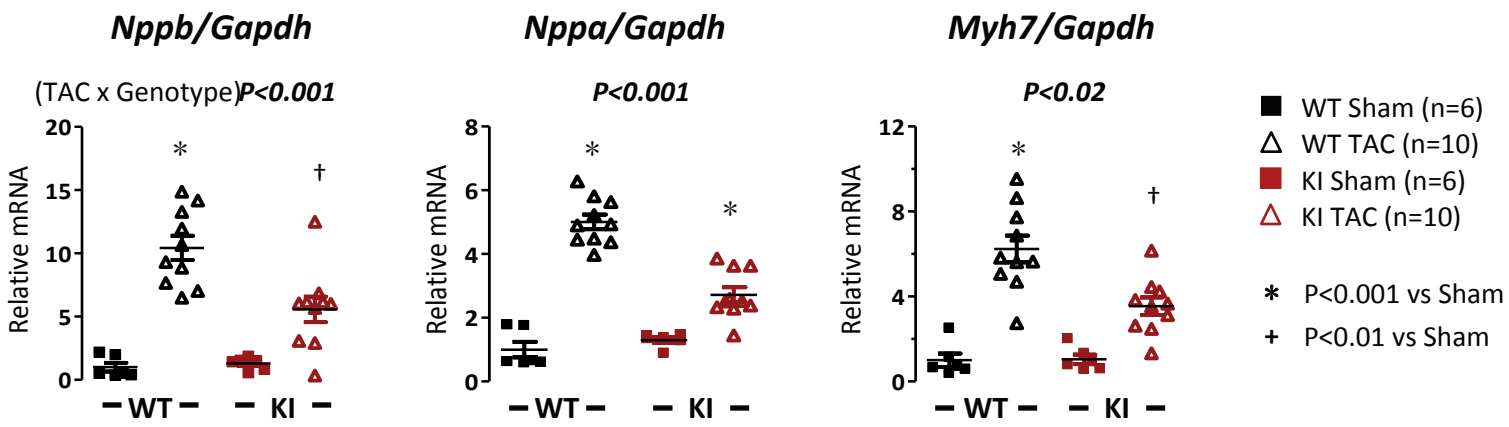
Nppb/Gapdh
(TAC x Genotype)P<0.001
Relative mRNA
20
15
10
5
0
*
†
WT
KI
Nppa/Gapdh
P<0.001
Relative mRNA
8
6
4
2
0
*
*
WT
KI
Myh7/Gapdh
P<0.02
Relative mRNA
12
8
4
0
*
†
WT
KI
WT Sham (n=6)
WT TAC (n=10)
KI Sham (n=6)
KI TAC (n=10)
* P<0.001 vs Sham
+ P<0.01 vs Sham

Figure S4

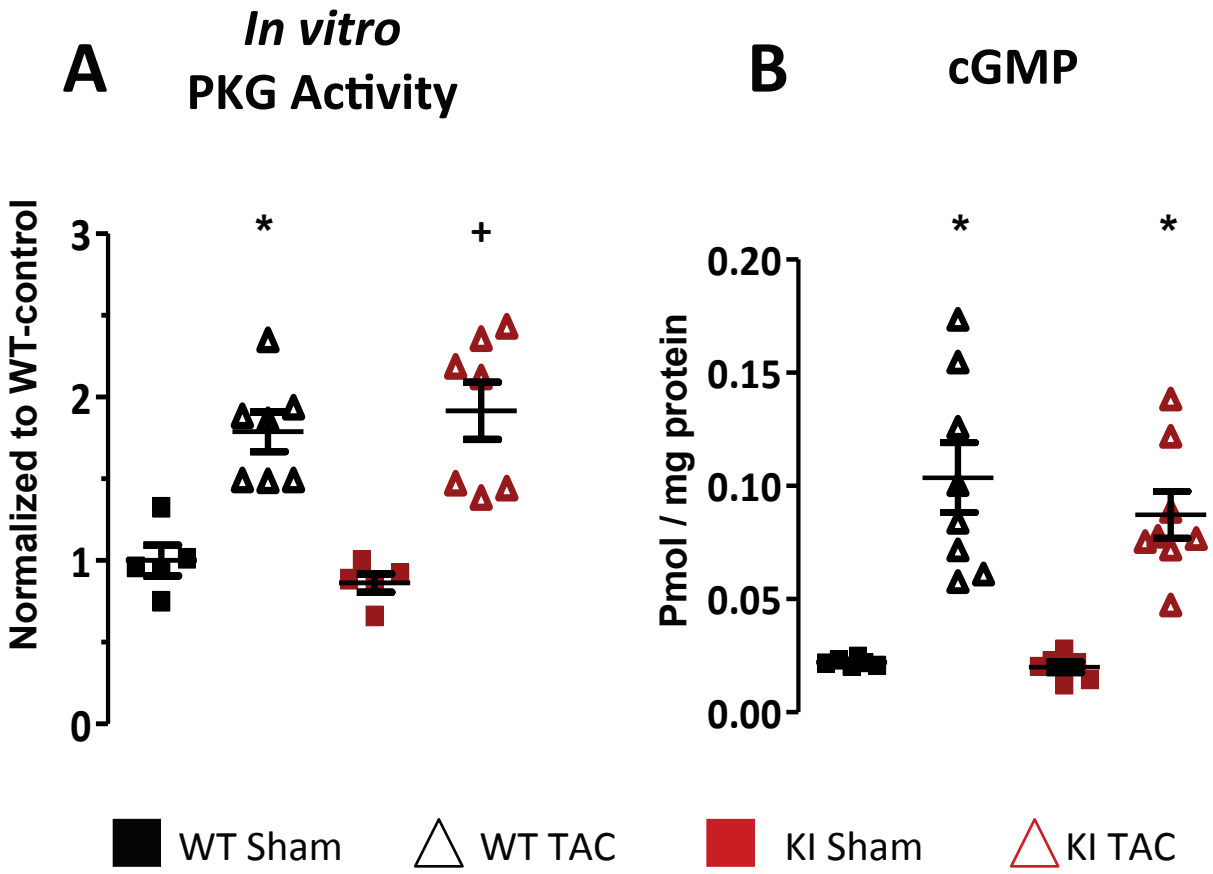
A
In vitro
PKG Activity
Normalized to WT-control
3
2
1
0
*
+
B
cGMP
Pmol / mg protein
0.20
0.15
0.10
0.05
0.00
*
*
WT Sham
WT TAC
KI Sham
KI TAC

Figure S5

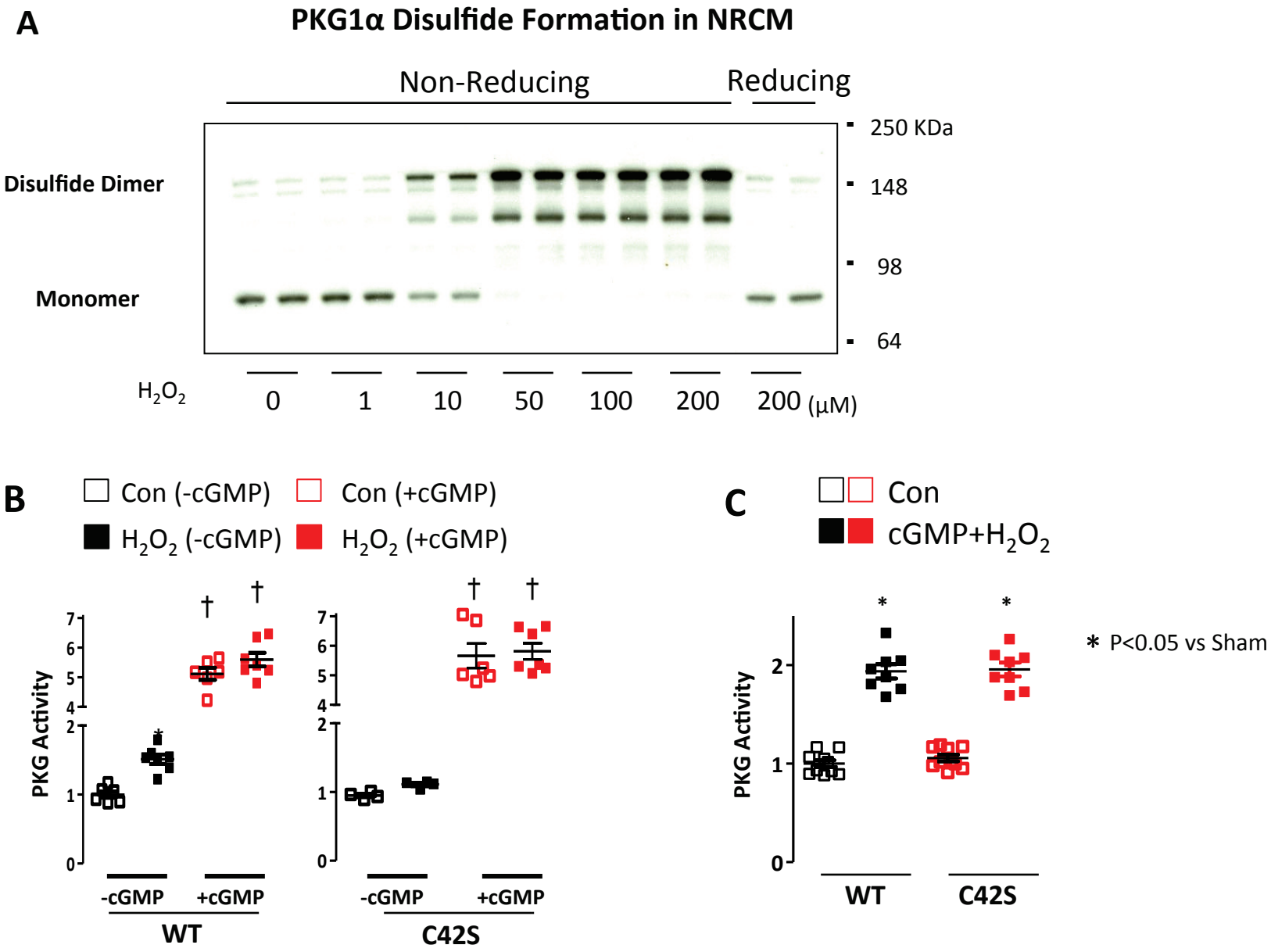
A
PKG1α Disulfide Formation in NRCM
Non-Reducing
Reducing
Disulfide Dimer
Monomer
250 KDa
148
98
64
H2O2
0
1
10
50
100
200
200 (μM)
B
Con (-cGMP)
Con (+cGMP)
H2O2 (-cGMP)
H2O2 (+cGMP)
PKG Activity
-cGMP
+cGMP
WT
C42S
C
Con
cGMP+H2O2
PKG Activity
WT
C42S
* P<0.05 vs Sham

Figure S6

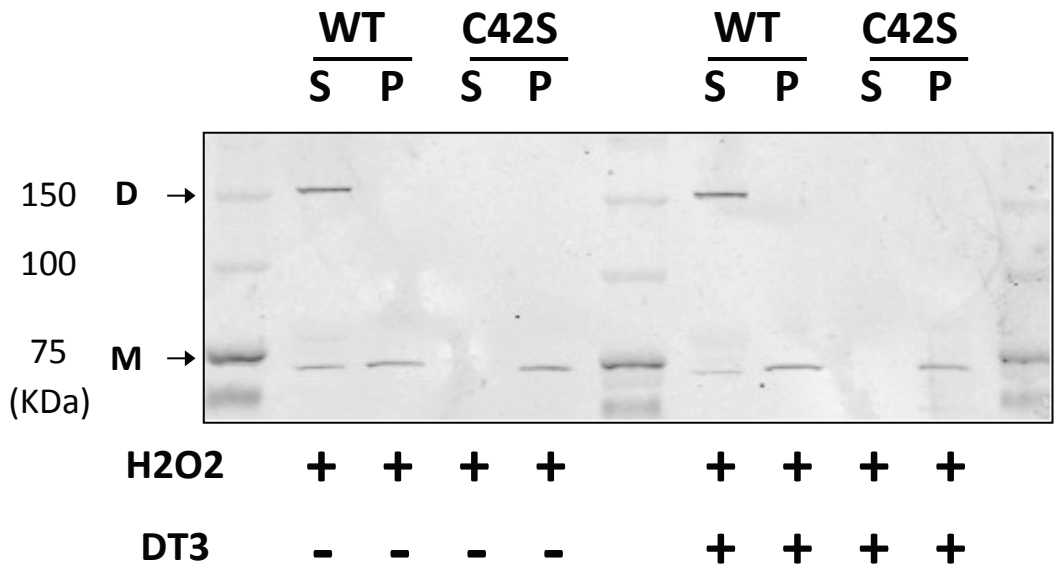

Figure S7

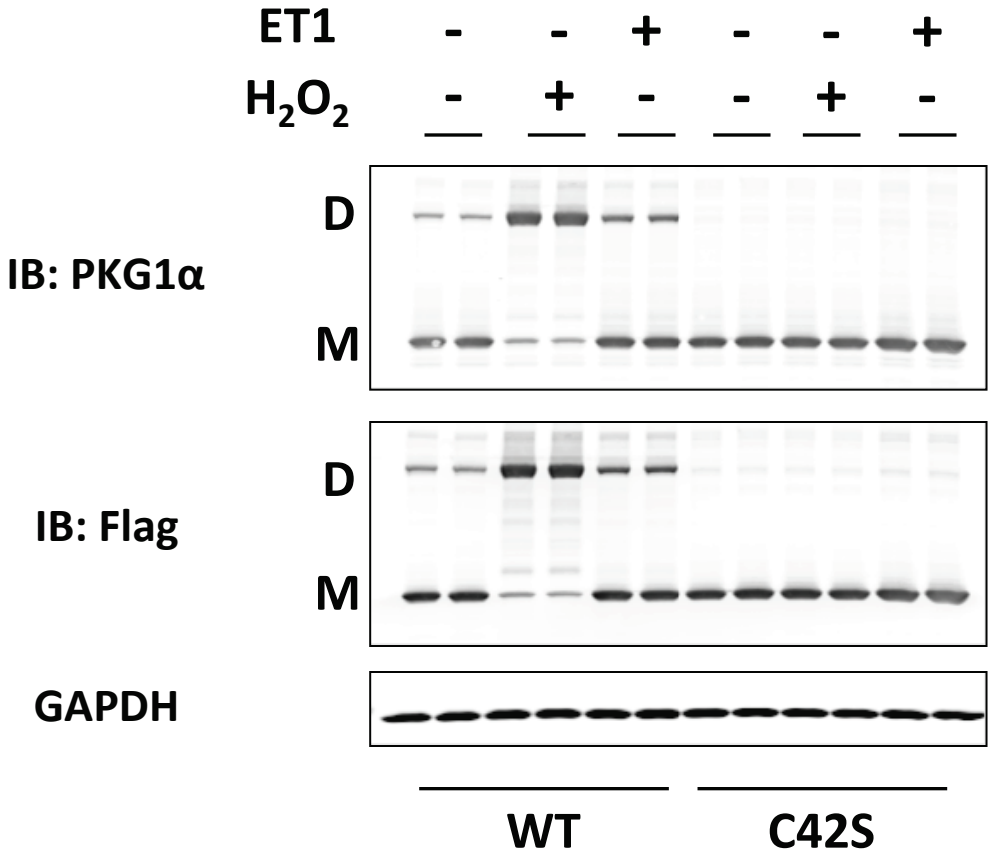

Revised Figure S8

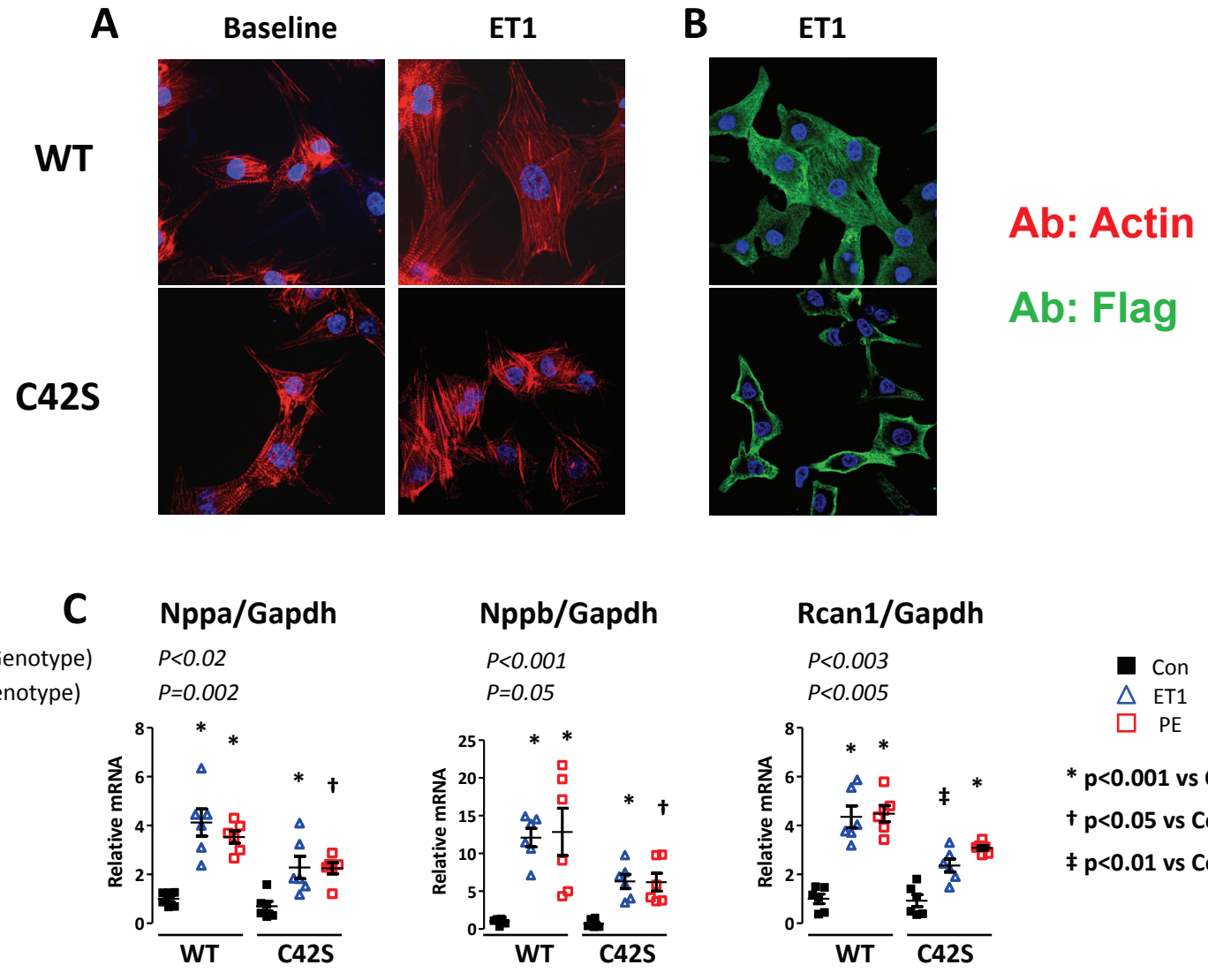
A
Baseline
ET1
B
ET1
WT
C42S
Ab: Actin
Ab: Flag
C
Nppa/Gapdh
Nppb/Gapdh
Rcan1/Gapdh
(ET1 x Genotype)
(PE x Genotype)
P<0.02
P=0.002
P<0.001
P=0.05
P<0.003
P<0.005
Relative mRNA
WT
C42S
Con
ET1
PE
* p<0.001 vs Con
† p<0.05 vs Con
‡ p<0.01 vs Con

Figure S9

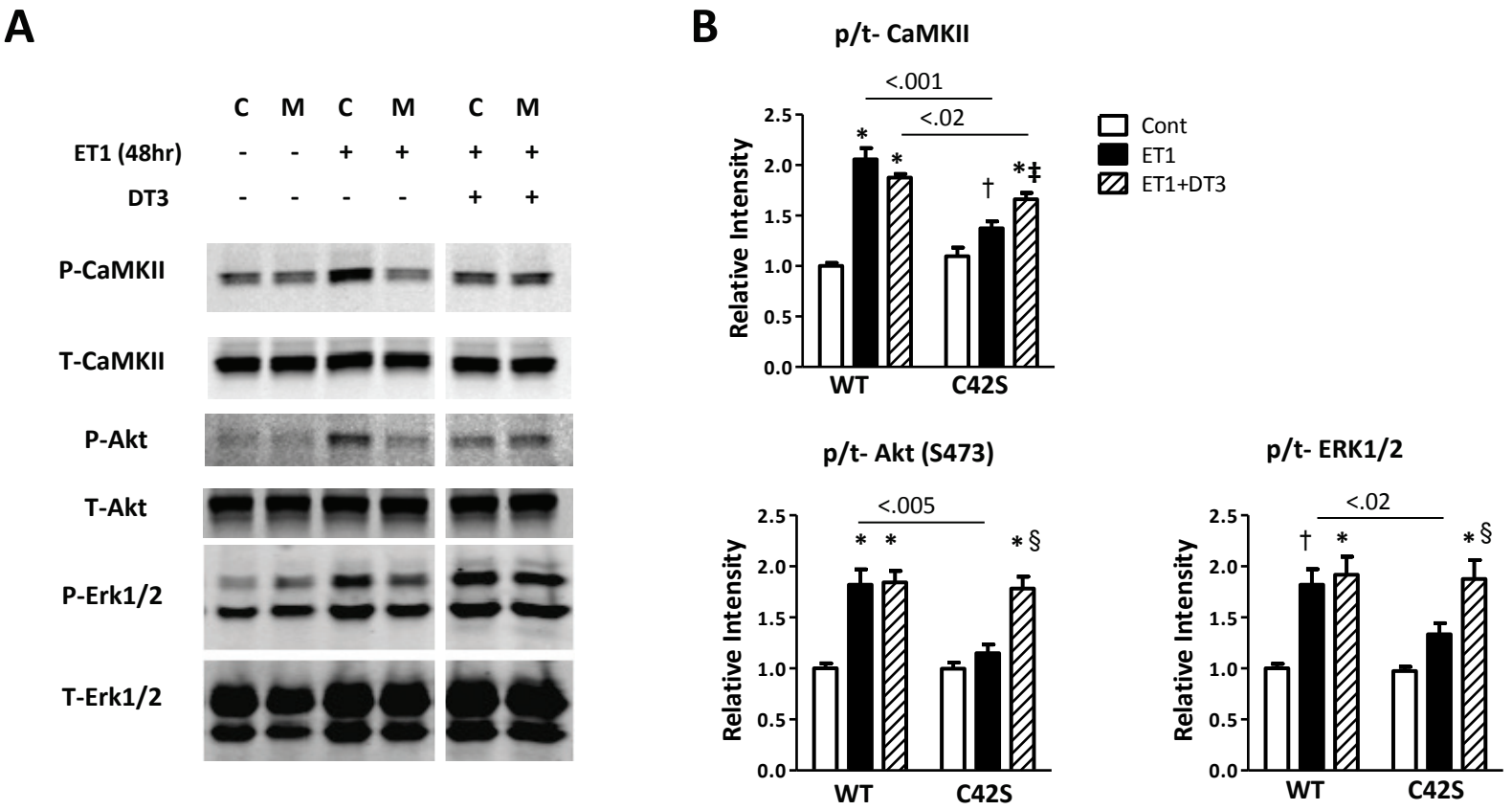
A
C M C M C M
ET1 (48hr) - - + + + +
DT3 - - - - + +
P-CaMKII
T-CaMKII
P-Akt
T-Akt
P-Erk1/2
T-Erk1/2
B
p/t- CaMKII
<.001
<.02
Cont
ET1
ET1+DT3
Relative Intensity
2.5
2.0
1.5
1.0
0.5
0.0
WT
C42S
p/t- Akt (S473)
<.005
p/t- ERK1/2
<.02

Figure S10

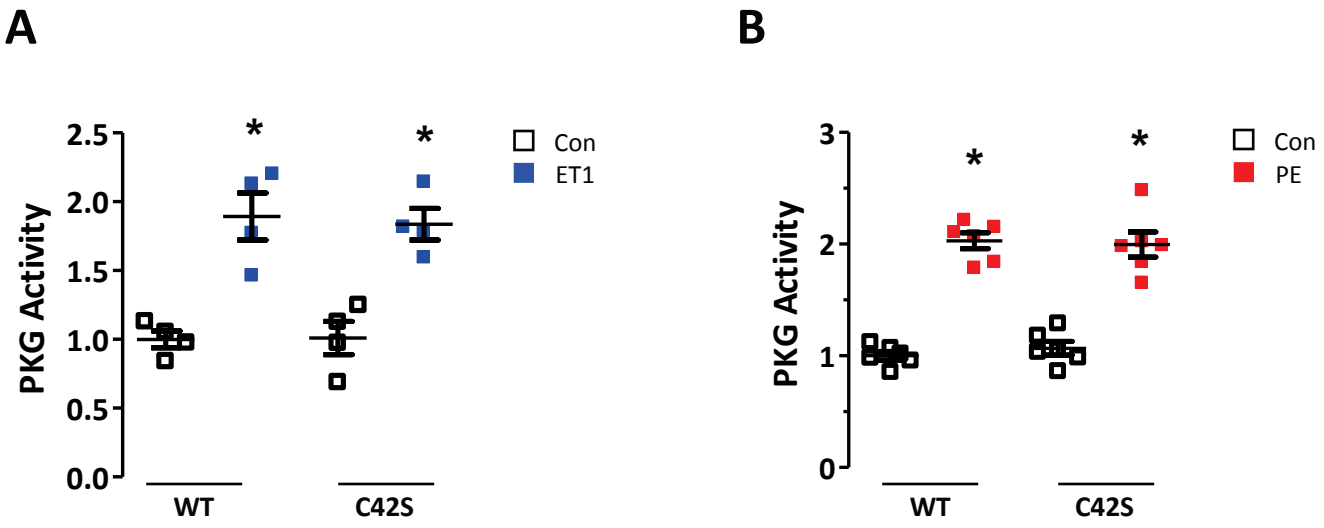
A
PKG Activity
2.5
2.0
1.5
1.0
0.5
0.0
*
*
Con
ET1
WT
C42S
B
PKG Activity
3
2
1
0
*
*
Con
PE
WT
C42S

Figure S11

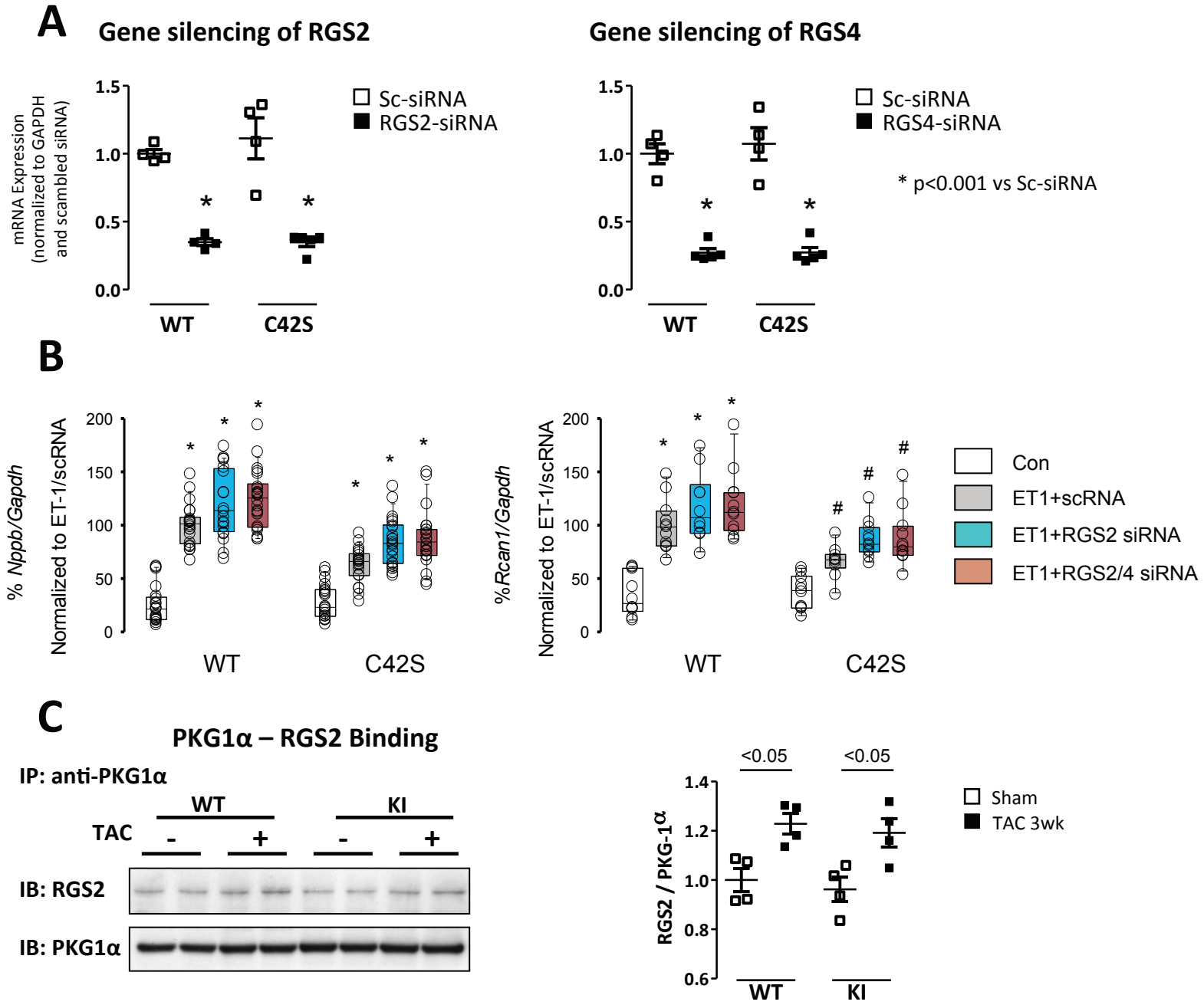
A
Gene silencing of RGS2
Gene silencing of RGS4
mRNA Expression (normalized to GAPDH and scambled siRNA)
Sc-siRNA
RGS2-siRNA
RGS4-siRNA
* p<0.001 vs Sc-siRNA
WT
C42S
B
% Nppb/Gapdh
%Rcan1/Gapdh
Normalized to ET-1/scRNA
Con
ET1+scRNA
ET1+RGS2 siRNA
ET1+RGS2/4 siRNA
C
PKG1α – RGS2 Binding
IP: anti-PKG1α
TAC
IB: RGS2
IB: PKG1α
KI
<0.05
RGS2 / PKG-1α
Sham
TAC 3wk

Figure S12

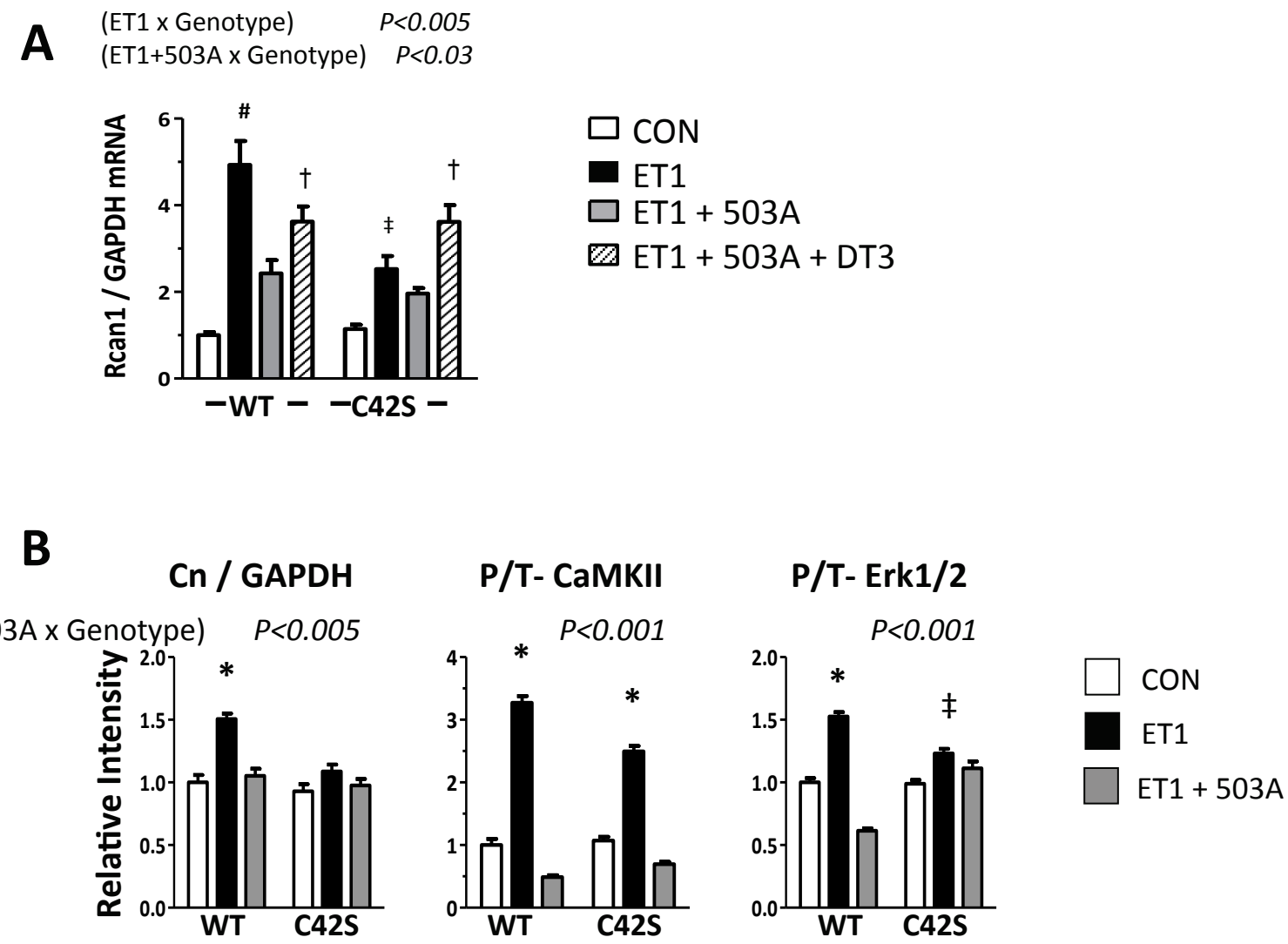
A
(ET1 x Genotype) P<0.005
(ET1+503A x Genotype) P<0.03
Rcan1 / GAPDH mRNA
WT
C42S
CON
ET1
ET1 + 503A
ET1 + 503A + DT3
B
Cn / GAPDH
P/T- CaMKII
P/T- Erk1/2
(ET1+503A x Genotype) P<0.005
P<0.001
P<0.001
Relative Intensity
WT
C42S
CON
ET1
ET1 + 503A

Figure S13

Supplemental Figure Legends:

S1) Representative non-reducing electrophoresis displaying PKG monomer and dimer in left ventricular myocardium from **A)** mouse pressure-overload hypertrophy (n=4/group) and **B)** canine atrial tachypaced-induced heart failure (n=5/group) (9). PKG1α disulfide dimer formation was increased in both stressed models compared to respective controls. Hearts expressing PKG1α^{C42S} (KI) showed monomer only. Percentage of dimeric PKG was compared by non-parametric test. *p<0.05 vs WT Sham, †p<0.02 vs Con. PKG monomer and disulfide dimer are abbreviated as M and D, respectively.

S2) Serial echocardiographic data for **A)** left intraventricular septum wall thickness, **B)** ejection fraction (EF), **C-D**) left ventricular end-systolic dimension (LVDs) and end-diastolic dimension (LVDd), and **E)** left ventricular mass. The number of animals studied for each group is shown. * p<0.005 vs sham. † p<0.01 vs sham. ‡ p<0.05, § p<0.005 by 2-way repeated measures ANOVA between KI PKG1α- and littermate controls (WT)-TAC groups.

S3) A) H&E staining and **B)** LV tissue weight/tibia length (TL) show greater hearts in WT versus KI PKG1 α after TAC. **C)** Wet lung weight corrected by body weight. The number of animals studied for each group is shown. * p<0.001 vs sham. P values shown in each figure are for the interaction term from a 2-way ANOVA with genotype (KI, littermate controls (WT) and +/- TAC as the categories.

S4) Expression of fetal genes induced by TAC. A and B-type natriuretic peptide (*Npp*a and *Nppb*) and β -myosin heavy chain (*Myh7*) are normalized to GAPDH (n=6: Sham, n=10: TAC).

* p<0.001 vs sham. p<0.01 vs sham. P values are for the interaction of TAC x Genotype based on 2-way ANOVA.

S5) Comparison of myocardial PKG activity after TAC between PKG genotype. **A)** *In vitro* myocardial PKG activity elevated similarly between WT-TAC and KI-TAC groups. Values were normalized to WT-Sham, (n=5:Sham, n=7:TAC group, *p<0.01, + p<0.001 vs sham). **B)** TAC similarly increased myocardial cGMP levels in both genotype (n=6:Sham, n=8:TAC, *p<0.001 vs sham).

S6) A) PKG1α disulfide dimer formation in response to varying doses of H_2O_2 (10 min incubation) in neonatal rat cardiomyocytes (NRCMs). An upper band (dimer) increased at a threshold dose of 10 μM H_2O_2, increasing at 50 and then reaching a plateau. Gel electrophoresis under reducing conditions is shown at the highest dose as a negative control. The lowest effective dose (10 μM) was used for the experiments based on these data.
B) Detection of altered PKG activity using an *in vitro* assay with or without cGMP in the reaction buffer. (n=4-6/group). Extracts were from NRCMs expressing either PKG1α^{WT}, or PKG1α^{C42S} and exposed to 10μM H_2O_2 for 15 minutes. H_2O_2 resulted in modest higher activity that was clearly detected if cGMP was not also added to the reaction buffer. If cGMP was added to the buffer (as done for the standard assay), PKG activity rose considerably, but was little altered by the addition of H_2O_2. † -p<0.01 vs assay run without cGMP added. Results of two-way ANOVA: (-cGMP: H_2O_2 effect p<0.006, + vs – cGMP: p<0.0001). Cells expressing the C42S mutant form of PKG1α displayed no effect from H_2O_2 (p>0.6), but also showed a significant rise in activity when cGMP was added to the assay buffer (p<0.0001). **C)** Myocytes pre-treated with H_2O_2 (10

μM) and cGMP (100 μM) in culture (15 minute incubation) prior to running the kinase activity assay (n=8-10/group). Here, the *in vitro* assay was run with cGMP added to the buffer, and normalized to data from non-stimulated control cells. PKG1α activity nearly doubled over baseline from H_2O_2+cGMP cell exposure, but this response was identical between PKG1α genotypes. This is similar to the results observed from cardiac tissue (e.g. Fig S5A).

S7) PKG redox modulation alters its subcellular compartmentation. Soluble (S) versus particulate (P) fractions from lysates of adult myocytes previously exposed to H_2O_2 for 60 minutes. Sub-fractionation protein gels were generated in non-reducing conditions. Disulfide PKG1α dimer was observed only in soluble fractions, whereas reduced PKG1α monomer could shift between membrane and particulate fractions. This distribution pattern was unaltered by co-incubation with selective PKG1α inhibitor DT3, so was independent of kinase activity. .

S8) NRCMs infected with adenovirus expressing either WT PKG1α or PKG1α^{C42S} were then exposed to either H_2O_2 (10 μM) for 10 minutes or ET1 (10 nM) for 48 hours. PKG1α dimer increased with both H_2O_2 and ET1 in cells expressing WT-PKG1α, but was not detected in cells expressing the PKG1α^{C42S}. The gels demonstrate that the dominant expressed form of PKG1α was provided by the transgene based on similar protein expression detected by Flag or PKG1α antibody.

S9) A) NRCMs exposed to 10 nM endothelin1 (ET1) for 48 hours develop a hypertrophic phenotype when the form of PKG1α expressed is WT (enhanced actin assessed by rhodamine phalloidin stain), but this is prevented if PKG1α^{C42S} is expressed. **B)** Intracellular localization of

exogenous PKG1α after ET1 exposure is diffuse in cells expressing the WT form, but intensifies at the plasma membrane in cells expressing PKG1α^{C42S}. **C)** Cells expressing WT-PKG1α exposed to 10 nM ET-1 or 10 μM PE for 48 hours display increased fetal gene expression (*Nppa*, *Nppb*) and regulator of calcineurin – 1 (*Rcan1*). This response was diminished in cells expressing PKG1α^{C42S}. N=6/group; * p<0.001; † p<0.05; ‡ p<0.01 vs respective control. P values in each panel are for the interaction term (ET1 x Genotype) and (PE x Genotype) from 2-way ANOVA.

S10) Calcium-calmodulin kinase II (CamKII), protein kinase B (PKB or Akt), and extracellular regulated kinase 1/2 (ERK 1/2) were activated by sustained ET-1 stimulation in rat neonatal myocytes expressing WT-PKG1α but less so in cells expressing PKG1α^{C42S}. Panel **A** shows example immunoblots (WT – wild-type PKG1α, M – C42S mutant form) which were run on the same gel but were noncontiguous, and panel **B** provides summary results. Addition of PKG inhibitor DT3 reversed the disparity between groups, confirming protection from PKG1α^{C42S} was due to PKG activity. n=6-8/group. 1-way ANOVA results: * p<0.001 versus respective control; † p<0.05 vs control; ‡ p<0.05 vs KI-ET-1; § p<0.001 vs KI-ET-1. P-values in figure are for post-hoc paired analysis of 2-way ANOVA.

S11) NRCMs exposed to 24 hours of **A)** ET-1 (n=4/group) or **B)** PE (n=6/group) show similar increases in total PKG assessed by *in vitro* assay with either WT or PKG1α^{C42S} expressed.
* p<0.01 vs respective control.

S12) A) Quantitative PCR results for RGS2 or RGS4 gene expression (normalized to GAPDH) in NRCMs transfected with siRNA against either gene. Data are shown for cells expressing WT or

C42S form of PKG1α. Gene silencing reduced expression by ~70% (n=4-5/group; * p<0.001). **B)** Hypertrophic gene expression (*Nppb* and *Rcan1*) normalized to *Gapdh* from NRCMs treated with ET-1 for 48 hours (n=10-11 in each group). Data are further normalized to the expression change produced by exposure to ET-1 + scrambled RNA (scRNA), which is set to a mean of 100%. Overall, expression rose somewhat more in cells in which RGS2 or RGS2 combined with RGS4 were suppressed by targeted siRNA (p<0.005 for *Nppb* and p<0.15 for *Rcan1* by 2-way ANOVA). There was also reduced expression of both genes in those cells expressing PKGα^{C42S} (p<0.001 for both), but we observed no interaction effect between PKG1α genotype and RGS2 or combined RGS2/4 gene silencing (p>0.7 for both genes). * p<0.001 vs control, # p<0.015 vs control. **C)** Immunoprecipitation of PKG1α probed for RGS2 and PKG1α in both WT- PKG1α and PKG1α^{C42S} expressing hearts with or without exposure to TAC (n=4/group). There was a slightly greater protein-protein interaction between PKG1α and RGS2 after TAC, but this was similar between groups.

S13) A) Additional analysis of NRCM experiment shown in Fig. 3C. ET1-induced increased *Rcan1* gene expression is blunted by TRPC3/6 blockade (503A) in NRCMs expressing WT-PKG1α, and this suppression is reversed by PKG-blocker - DT3. Cells expressing PKG1α^{C42S} show a reduced response to ET1 and no impact by 503A, but DT3 removes the protective effect from PKG1α^{C42S}. # p<0.001 vs CON and ET1+503A, † p<0.05 vs ET1+503A, ‡ p<0.05 vs CON. P-values are for interaction term of 2-way ANOVA: ET-1 x Genotype; and ET-1+503A x Genotype. (n=7: CON, n=7-8: ET1, n=6: ET1+503A, n=3: ET1+503A+DT3). **B)** Summary data for protein analysis in RNCM study shown in Figure 3D. Data are normalized to PKG1α-WT expressing controls. Cn-calcineurin; CaMKII – Calcium calmodulin dependent Kinase II, ERK1/2 (extracellular response

kinase 1/2). Data were measured from RNCM extracts obtained after 48-hrs ET1 stimulation ±TRPC3/6 inhibition (n=6/group); * $p<0.001$ vs other groups, ‡ $p<0.001$ vs CON.

References:

1. Prysyazhna, O., Rudyk, O., and Eaton, P. 2012. Single atom substitution in mouse protein kinase G eliminates oxidant sensing to cause hypertension. *Nat Med* 18:286-290.
2. Takimoto, E., Champion, H.C., Li, M., Belardi, D., Ren, S., Rodriguez, E.R., Bedja, D., Gabrielson, K.L., Wang, Y., and Kass, D.A. 2005. Chronic inhibition of cyclic GMP phosphodiesterase 5A prevents and reverses cardiac hypertrophy. *Nat.Med.* 11:214-222.
3. Liang, Q., Carlson, E.C., Donthi, R.V., Kralik, P.M., Shen, X., and Epstein, P.N. 2002. Overexpression of metallothionein reduces diabetic cardiomyopathy. *Diabetes* 51:174-181.
4. Yamamoto, M., Yang, G., Hong, C., Liu, J., Holle, E., Yu, X., Wagner, T., Vatner, S.F., and Sadoshima, J. 2003. Inhibition of endogenous thioredoxin in the heart increases oxidative stress and cardiac hypertrophy. *J Clin Invest* 112:1395-1406.
5. Rudyk, O., Phinikaridou, A., Prysyazhna, O., Burgoyne, J.R., Botnar, R.M., and Eaton, P. 2013. Protein kinase G oxidation is a major cause of injury during sepsis. *Proc Natl Acad Sci U S A* 110:9909-9913.
6. Zhang, M., Takimoto, E., Hsu, S., Lee, D.I., Nagayama, T., Danner, T., Koitabashi, N., Barth, A.S., Bedja, D., Gabrielson, K.L., et al. 2010. Myocardial remodeling is controlled by myocyte-targeted gene regulation of phosphodiesterase type 5. *J Am Coll Cardiol* 56:2021-2030.
7. Takimoto, E., Koitabashi, N., Hsu, S., Ketner, E.A., Zhang, M., Nagayama, T., Bedja, D., Gabrielson, K.L., Blanton, R., Siderovski, D.P., et al. 2009. Regulator of G protein signaling 2 mediates cardiac compensation to pressure overload and antihypertrophic effects of PDE5 inhibition in mice. *J Clin Invest* 119:408-420.
8. Koitabashi, N., Aiba, T., Hesketh, G.G., Rowell, J., Zhang, M., Takimoto, E., Tomaselli, G.F., and Kass, D.A. 2010. Cyclic GMP/PKG-dependent inhibition of TRPC6 channel activity and expression negatively regulates cardiomyocyte NFAT activation Novel mechanism of cardiac stress modulation by PDE5 inhibition. *J Mol Cell Cardiol* 48:713-724.
9. Chakir, K., Depry, C., Dimaano, V.L., Zhu, W.Z., Vanderheyden, M., Bartunek, J., Abraham, T.P., Tomaselli, G.F., Liu, S.B., Xiang, Y.K., et al. 2011. Galphas-biased beta2-adrenergic receptor signaling from restoring synchronous contraction in the failing heart. *Sci Transl Med* 3:100ra188.